E-proceedings of the 36th IAHR World Congress
28 June – 3 July, 2015, The Hague, the Netherlands

Manning's coefficient of alternatively arranged sandbars with tree vegetation

KOHJI MICHIOKU [(1)], KEIICHI KANDA [(2)] SHUNICHI KOMETANI [(3)], YOSHIYUKI IRIE [(4)] & CHINAMI SAKAMOTO [(4)]

[(1)] Department of Civil and Environmental Engineering, Hosei University, Tokyo, Japan,
e-mail: kohji.michioku.47@hosei.ac.jp

[(2)] Department of Civil Engineering, National Institute of Technology, Akashi College, Akashi, Japan,
e-mail: kanda@akashi.ac.jp

[(3)] Graduate School of Engineering, Kobe University, Kobe, Japan,
e-mail: komesu5517@gmail.com

[(4)] Department of Civil Engineering, National Institute of Technology, Akashi College, Akashi, Japan,
e-mail: yossy-icochan@hotmail.co.jp

[(5)] Department of Civil Engineering, National Institute of Technology, Akashi College, Akashi, Japan,
e-mail: c1021@s.akashi.ac.jp

ABSTRACT

Recently, many river channels tend to be densely vegetated due to regime shifts in hydrological, fluvial and ecological processes. It is a critical engineering issue for flood control and management to evaluate the conveyance capacity of vegetated channels. In this study, an equivalent Manning's coefficient n_v of vegetation canopy drag in an open channel of compound cross section with alternatively arranged floodplain is analyzed by using a two-dimensional two-layer (2D2L) model. It is found that n_v monotonically increases with increasing discharge when vegetation is emerged. On the other hand, n_v gradually decreases with discharge in the case of submergent vegetation. The numerical solutions of flow structure and n_v is compared with experimental data to verify the model and satisfactory agreement between the analysis and the experiment is recognized.

Keywords: Manning roughness coefficient, vegetated channel, compound cross section, alternative bar

1. INTRODUCTION

Overgrowing woody vegetation or forestation in the river channels is a world-wide issue in many restored river channels, which decreases flow conveyance capacity and eventually increases the risk potential of flood disasters. From a viewpoint of flood control and management, the critical issue is how to determine conveyance capacity of vegetated channels. So far, many researchers have investigated hydrodynamics and ecologies in vegetated channels by laboratory and field measurements. Studies such as Nepf (1999) and Nikora and Nikora (2007) contributed in finding a functional dependency of the drag force coefficient C_D of plants on their density, height and stem diameter. In most hydraulic models for vegetated channels, flow resistance caused by vegetation canopy is approximated by an additional drag force or an increased bed roughness. Although C_D is a parameter widely used in analyzing hydrodynamics of vegetated rivers, it is not always a handy parameter from a practical viewpoint, since vegetation drag depends not only on vegetation properties but also on hydraulic parameters such as water depth and discharge. On the other hand, the high water level, HWL, for a design flood discharge is generally determined by performing one-dimensional analysis, where Manning's roughness coefficient is a key hydraulic parameter. Manning's roughness coefficient is the most convenient and authorized concept for describing vegetation canopy drag from the viewpoints of making river channel design and responding to public accountability requirement.

Wu et al. (1999), Green (2005), Nikora et al. (2008), De Doncker et al. (2009), Folkard (2011), Luhar and Nepf (2013) carried out extensive studies in order to precisely evaluate Manning's roughness coefficient n_V of vegetation canopy. When the drag force is described by n_V, how n_V depends on hydraulic and vegetational conditions must be properly evaluated, since the flow resistance mechanism tremendously changes with vegetation submergence ratio. Luhar and Nepf (2013) proposed an analytical solution for a functional dependency of n_V on water depth both for emerged and submerged vegetation. The authors proposed a two-dimensional two-layer model to analyze hydrodynamics in vegetated channels. The model is termed "2D2L Model", hereafter. Dividing the flow control volume vertically into the upper and lower layers at an interface encompassing the canopy top, mass and momentum conservations are formulated with respect to the fast flow over the vegetation and the slow flow through the porous vegetation. Mass and momentum exchange between the two layers are considered in order to describe internal shear layers developing at the two layer interface. This model is more advantageous than any other shallow flow models in describing hydrodynamics of submerged vegetation. The 2D2L model was already applied to flood flow analysis in vegetated rivers (Michioku et al., 2008). In order to examine dependency of n_V on hydraulic and vegetational conditions, Michioku et al. (2014) applied the model to examine hydrodynamics in a straight channel of compound cross section with floodplain vegetation. A functional dependency of n_V on vegetation properties such as vegetation structure, stem diameter and height of vegetation, etc. was investigated and a laboratory experiment was conducted to verify the model. It was found that n_V

monotonically increases with increasing discharge for an emergent vegetation, whilst it becomes less dependent on discharge for submerged vegetation.

It is frequently observed that vegetation tends to be overgrown on alternative sandbars or meandering channels rather than in straight channels. In this study, focusing on these configurations of vegetation and channel morphology, the 2D2L model was applied to analyze hydrodynamics in an open channel of compound channel with vegetated alternative sandbar or floodplain. How the equivalent Manning's roughness coefficient, n_V, depends on vegetational and hydraulic conditions was investigated. In addition, a laboratory experiment was carried out in an open channel with alternatively arranged vegetation in order to compare the flow structure and n_V with the numerical results of the 2D2L model.

2. FLOW ANALYSIS

2.1 Two-dimensional two-layer model: 2D2L model

Figure 1 schematically indicates a flow configuration in a river with tree-vegetated floodplain. The domain consists of non-vegetated and vegetated areas, where they are defined as "Domain-A" and "Domain-B", respectively. As shown in Figure 1 the whole flow system is vertically divided into two layers by an interface that encompasses the canopy top. Mass and momentum conservation are formulated in layer-averaged forms. The system is two-layered not only in the vegetated area but also in the non-vegetated area so that the interfacial shear layer developing behind the bush could be reproduced. Since momentum is exchanged between the two layers with distance departing from the vegetation, the two-layer flow asymptotically approaches a single-layer flow in the stream-wise direction. Although sedimentation is not considered in this study, the concept of a two-layer structure is available also in the movable river bed.

2.2 Equation of continuity and entrainment velocity

A layer-integrated two-dimensional equation system is formulated. Mass conservation for the upper and lower layers are written for a two-layer control volume as

$$\frac{\partial h_{\mathrm{m}}}{\partial t}+\frac{\partial M_{\mathrm{m}}}{\partial x}+\frac{\partial N_{\mathrm{m}}}{\partial y}=-\Gamma_{\mathrm{m}} q_{\mathrm{i}} \qquad [1]$$

where t: time coordinate, (x, y): Cartesian space coordinates, m(=1,2): a subscript indicating the layers, ($M_m=u_m h_m$, $N_m=v_m h_m$): discharge fluxes in the x and y directions, (u_m, v_m): layer-averaged velocity vectors, h_m: layer thickness ($h_1=h_V$, $h_2=h-h_1$), h: total water depth, h_V: vegetation height and q_i: entrainment velocity across the two-layer interface. Γ_m is a switching parameter to distinguish the layers as

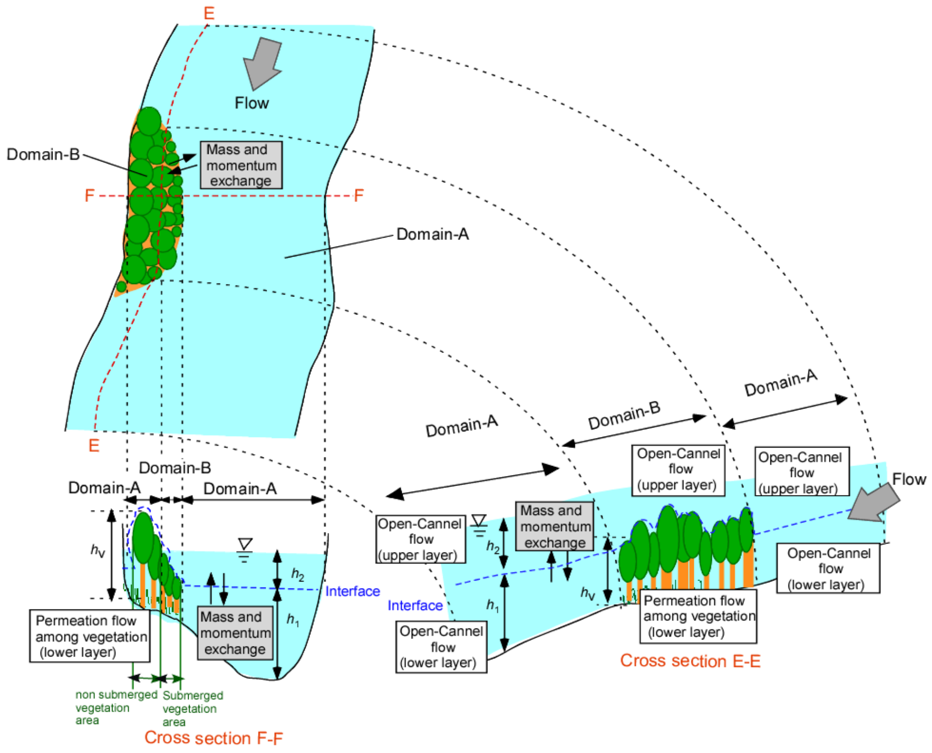

Figure 1. Flow configuration of the 2D2L model

$$\Gamma_{\mathrm{m}} = \begin{cases} 1 & m=1 \quad \text{for the lower layer} \\ -1 & m=2 \quad \text{for the upper layer} \end{cases} \tag{2}$$

Since the lower layer thickness, h_1=h_V is constant independently of time, Eq.[1] leads to a solution of the entrainment velocity q_i as

$$q_{\mathrm{i}} = -\left(\frac{\partial M_1}{\partial x} + \frac{\partial N_1}{\partial y}\right) \tag{3}$$

These formulations are the same both in Domains-A and B

2.3 Momentum equations

The momentum conservation in Domain-A or on the vegetation-less domain is formulated as

$$\frac{\partial}{\partial t}\begin{bmatrix} M_{\mathrm{m}} \\ N_{\mathrm{m}} \end{bmatrix} + \frac{\partial}{\partial x}\left\{u_{\mathrm{m}}\begin{bmatrix} M_{\mathrm{m}} \\ N_{\mathrm{m}} \end{bmatrix}\right\} + \frac{\partial}{\partial y}\left\{v_{\mathrm{m}}\begin{bmatrix} M_{\mathrm{m}} \\ N_{\mathrm{m}} \end{bmatrix}\right\} = -gh_{\mathrm{m}}\begin{bmatrix} \partial/\partial x \\ \partial/\partial y \end{bmatrix} z_{\mathrm{S}} + \frac{\partial}{\partial x}\begin{bmatrix} -\overline{u_{\mathrm{m}}'^2}h_{\mathrm{m}} \\ -\overline{v_{\mathrm{m}}'u_{\mathrm{m}}'}h_{\mathrm{m}} \end{bmatrix} + \frac{\partial}{\partial y}\begin{bmatrix} -\overline{u_{\mathrm{m}}'v_{\mathrm{m}}'}h_{\mathrm{m}} \\ -\overline{v_{\mathrm{m}}'^2}h_{\mathrm{m}} \end{bmatrix}$$
$$\underbrace{-\frac{\delta_{\mathrm{m1}}^{\mathrm{A}}}{\rho}\begin{bmatrix} \tau_{\mathrm{b}}^{\mathrm{x}} \\ \tau_{\mathrm{b}}^{\mathrm{y}} \end{bmatrix}}_{\text{Bed shear stress}} \underbrace{+\Gamma_{\mathrm{m}}Eq_{\mathrm{i}}\begin{bmatrix} u_2-u_1 \\ v_2-v_1 \end{bmatrix} - \Gamma_{\mathrm{m}}\begin{bmatrix} u_{\mathrm{i}} \\ v_{\mathrm{i}} \end{bmatrix}q_{\mathrm{i}}}_{\text{Interfacial stress}} \tag{4}$$

where g: gravity acceleration, z_S: water surface elevation, $\delta^{\mathrm{A}}_{\mathrm{m1}}$: a delta function in which $\delta^{\mathrm{A}}_{\mathrm{m1}}$=1 in Domain-A's lower layer and $\delta^{\mathrm{A}}_{\mathrm{m1}}$=0 elsewhere, ($\tau_{\mathrm{b}}^{\mathrm{x}}, \tau_{\mathrm{b}}^{\mathrm{y}}$): bed shear stress vectors in the (x, y) directions, ($-\overline{u_{\mathrm{m}}'v_{\mathrm{m}}'}, -\overline{u_{\mathrm{m}}'^2}, -\overline{v_{\mathrm{m}}'^2}$): layer-averaged Reynolds stresses, ρ: water density and (u_i, v_i): interfacial velocity vectors. ($\tau_{\mathrm{b}}^{\mathrm{x}}, \tau_{\mathrm{b}}^{\mathrm{y}}$) are given in terms of the Manning's coefficient n_0 as

$$(\tau_{\mathrm{b}}^{\mathrm{x}}, \tau_{\mathrm{b}}^{\mathrm{y}}) = \frac{\rho g n_0^2\sqrt{u^2+v^2}}{h^{1/3}}(u,v) \tag{5}$$

where (u, v) are depth-averaged velocity components defined by

$$\begin{bmatrix} u \\ v \end{bmatrix} = \left(\begin{bmatrix} u_1 \\ v_1 \end{bmatrix}h_1 + \begin{bmatrix} u_2 \\ v_2 \end{bmatrix}h_2\right)/h \tag{6}$$

The layer averaged Reynolds stresses in Eq.[4] are formulated by means of the zero-order turbulence closure as

$$-\overline{u_{\mathrm{m}}'^2} = 2D_{\mathrm{h}}\left(\frac{\partial u_{\mathrm{m}}}{\partial x}\right) - \frac{2}{3}k_{\mathrm{m}},\ -\overline{v_{\mathrm{m}}'u_{\mathrm{m}}'} = D_{\mathrm{h}}\left(\frac{\partial u_{\mathrm{m}}}{\partial y} + \frac{\partial v_{\mathrm{m}}}{\partial x}\right),\ \ -\overline{v_{\mathrm{m}}'^2} = 2D_{\mathrm{h}}\left(\frac{\partial v_{\mathrm{m}}}{\partial y}\right) - \frac{2}{3}k_{\mathrm{m}} \tag{7}$$

The horizontal eddy viscosity D_h in Eq.[7] is proportional to the product of local water depth h and friction velocity of bed shear stress u_* as D_h=α_D hu_*, where α_D =0.3 as recommended by Hosoda et al. (1996). The layer-averaged turbulent kinetic energy, $k_{\mathrm{m}} = (\overline{u_{\mathrm{m}}'^2} + \overline{v_{\mathrm{m}}'^2} + \overline{w_{\mathrm{m}}'^2})/2$, is given by a semi-empirical formula proposed by Nezu and Nakagawa(1993).

The internal shear stress acting on the two-layer interface is described in terms of an entrainment velocity q_i. Considering the direction of momentum exchange across the two-layer interface, the parameter E is defined as

$$E = \begin{cases} 1 & q_{\mathrm{i}} > 0 \quad \text{(upward mass transfer)} \\ -1 & q_{\mathrm{i}} < 0 \quad \text{(downward mass transfer)} \end{cases} \tag{8}$$

In Domain-B or in the vegetated area, the velocity and discharge fluxes in the lower layer, (u_1, v_1) and (M_1, N_1), are replaced by (u_S, v_S), and (M_S, N_S), respectively, where, the subscript "S" represents the apparent component of variables. The momentum equation for the upper layer is the same as Eq.[4]. The lower layer consisting of water and vegetation is modeled as a porous body in the same manner as the flow in permeable rubble-mound (Michioku et al., (2005)). The equation is formulated as

$$\frac{\partial}{\partial t}\begin{bmatrix} M_{\mathrm{m}} \\ N_{\mathrm{m}} \end{bmatrix} + \frac{\partial}{\partial x}\left\{u_{\mathrm{m}}\begin{bmatrix} M_{\mathrm{m}} \\ N_{\mathrm{m}} \end{bmatrix}\right\} + \frac{\partial}{\partial y}\left\{v_{\mathrm{m}}\begin{bmatrix} M_{\mathrm{m}} \\ N_{\mathrm{m}} \end{bmatrix}\right\} = -gh_{\mathrm{V}}\begin{bmatrix} \partial/\partial x \\ \partial/\partial y \end{bmatrix} z_{\mathrm{S}} + \frac{\partial}{\partial x}\begin{bmatrix} -\overline{u'^2_{\mathrm{m}}}h_{\mathrm{V}} \\ -\overline{v'_{\mathrm{m}}u'_{\mathrm{m}}}h_{\mathrm{V}} \end{bmatrix} + \frac{\partial}{\partial y}\begin{bmatrix} -\overline{u'_{\mathrm{m}}v'_{\mathrm{m}}}h_{\mathrm{V}} \\ -\overline{v'^2_{\mathrm{m}}}h_{\mathrm{V}} \end{bmatrix}$$
$$\underbrace{-\frac{\delta^{\mathrm{B}}_{\mathrm{m1}}}{\rho}\begin{bmatrix} \tau^{\mathrm{x}}_{\mathrm{b}} \\ \tau^{\mathrm{y}}_{\mathrm{b}} \end{bmatrix}}_{\text{Bed shear stress}} \underbrace{-\frac{\delta^{\mathrm{B}}_{\mathrm{m1}}}{\rho}\begin{bmatrix} F_{\mathrm{x}} \\ F_{\mathrm{y}} \end{bmatrix}}_{\text{Drag force}} \underbrace{+\Gamma_{\mathrm{m}}Eq_{\mathrm{i}}\begin{bmatrix} u_2-u_1 \\ v_2-v_1 \end{bmatrix}}_{\text{Interfacial shear stress}} - \Gamma_{\mathrm{m}}\begin{bmatrix} u_{\mathrm{i}} \\ v_{\mathrm{i}} \end{bmatrix} q_{\mathrm{i}} \qquad [9]$$

where $\delta^{\mathrm{B}}_{\mathrm{m1}}$: a delta function in which $\delta^{\mathrm{B}}_{\mathrm{m1}}$ =1 in Domain-B's lower layer and $\delta^{\mathrm{B}}_{\mathrm{m1}}$ =0 elsewhere.

The flow resistance in the vegetation consists of three components as in Eq.[9], which are the bed shear stress, the drag force and the interfacial shear stress mentioned above. The bed shear stress is acting on the forest floor and described in terms of Manning's roughness coefficient n_0. The drag forces (F_x, F_y) imposed on the vegetation are modeled as

$$(F_{\mathrm{x}}, F_{\mathrm{y}}) = \frac{\rho C_{\mathrm{D}}\lambda_{\mathrm{veg}}h_{\mathrm{V}}\sqrt{u_1^2+v_1^2}}{2}(u_1, v_1) \qquad [10]$$

The drag force coefficient C_D is given as functions of vegetation parameters such as vegetation density λ_{veg}, stem diameter d, height h_V and spacing ΔS of the trees. According to Nepf (1999), the roughness density of vegetation λ_{veg} is equivalent to the projected plant area per unit volume as

$$\lambda_{veg}=D/\Delta S^2 \qquad [11]$$

Here, the tree is assumed to be a rigid cylinder and other willow properties such as flexibility, profile, foliage are not considered in the present analysis.

3. LABORATORY EXPERIMENT

3.1 Summary of experimental setup

A laboratory experiment was carried out in order to verify the numerical analysis. The test flume is 8m in length and 1m in width that is equipped in a hydraulic laboratory in the National Institute of Technology, Akashi College. The channel's bed slope was fixed to be 1/1,000. Although the open channel examined in this study has alternatively arranged sandbars with vegetation, the experimental channel has a little simplified configuration of a single cross section with the alternatively arranged vegetation. The floodplain or sandbar is absent in the experimental system and the channel has a single rectangular cross section, since the main focus in the laboratory experiment is placed on vegetation hydrodynamics rather than on channel geometry.

4.5 times wave interval of triangular vegetation alternatively were arranged along 6.9m long reach as shown in Figure 2. The tree vegetation models are inflexible wooden cylinders with a diameter of d=1.2cm in staggered rows. As listed in Table 1, vegetation height is h_V=6.0cm, plant spacing is ΔS=10.95cm and vegetation density or tree number per unit bed area is N_V=0.00834 cm^{-2}. Accordingly, the roughness density of vegetation is λ_{veg} =0.01 cm^{-1} as defined in Eq[11]. Photo 1 shows an overview of the experimental setup. The experiment was carried out for discharge between Q_0=8.10~35.87l/s. This range of discharge covers vegetational conditions from emergent to submergent vegetation. A steady uniform flow condition was established by adjusting the movable weir equipped at the downstream end. The uniform flow water depth, h_0, was determined from measurement at several points along the stream.

Table 1. Experimental conditions.

Stem diameter d (cm)	Vegetation height h_V (cm)	Spacing of plant ΔS (cm)	Vegetation density N_V (1/cm^2)	Roughness density of vegetation λ_{veg} (cm^{-1})
1.2	6	10.95	0.00834	0.01

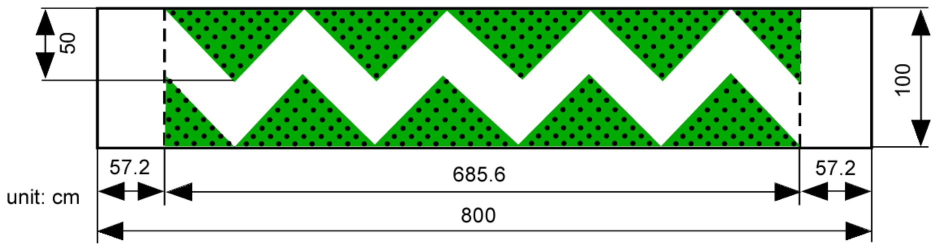

Figure 2. Plane view of alternatively arranged vegetation in the test flume.

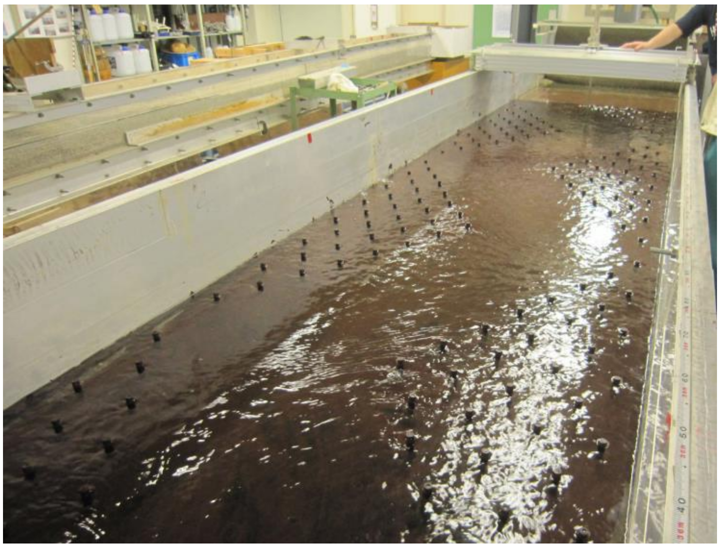

Photo 1. Overview of test flume with vegetation models.

3.2 Comparison of rating curve and Manning's roughness coefficient between experiment and theory

After a uniform flow condition is established, the Manning's roughness coefficient N_1 is calculated from the measured water depth h_0 and discharge Q_0 by using the following formula.

$$N_1 = \frac{R_0^{2/3} \cdot I^{1/2} \cdot A_0}{Q_0} \qquad [12]$$

where A_0: cross-sectional area, R_0: hydraulic radius and I: channel bed slope. The subscript "0" denotes values for uniform flow condition.

N_1 is termed "Manning's roughness coefficient calculated from real flow", hereafter. Analytical value for N_1 can be computed from the 2D2L model by using Eq.[12] in the same manner. Note that n_0 =0.012m$^{-1/3}$s is given as a boundary roughness coefficient for the test flume in the analysis.

In Figure 3, the experimental results for rating curve, (h_0, Q_0) and Manning's roughness coefficient N_1 are compared with the analytical solutions from the 2D2L hydrodynamic model. The model agrees with the experiment for wide range of water depth from emergent to submergent vegetation. It is confirmed from the figure that the hydrodynamics in the experiment can be correctly described by the 2D2L model.

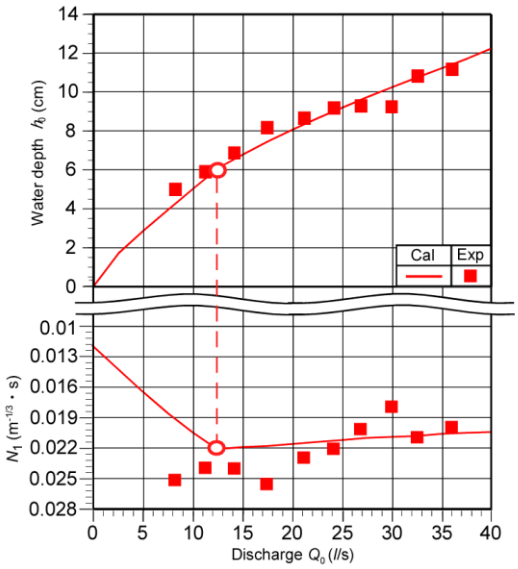

Figure 3. Uniform flow water depth h_0 and Manning's roughness coefficient N_1 against discharge Q_0. N_1 is the roughness factor calculated from real flows in the experiment and numerical analysis. Symbols are experimental data. Solid lines represent theoretical solutions from the 2D2L model. The open circle corresponds to a point of vegetation submergence.

4. EQUIVALENT MANNING'S ROUGHNESS COEFFICIENT OF VEGETATION CANOPY DRAG: n_V

4.1 Definition of n_V

Consider an open channel of compound cross section with vegetation on alternatively arranged sandbar or floodplain as shown in Figure 4(a). In the 2D2L model, the system is vertically divided into two layers by a horizontal interface encompassing the canopy top. According to Eq.[10], the drag force generated by vegetation is described in terms of the lower layer velocity U_1 as

$$F_V = \frac{1}{2} C_D \rho \lambda_{veg} U_1^2 h_v \qquad [13]$$

where C_D: drag force coefficient and h_V: vegetation height. The roughness density λ_{veg} is given by

$$\lambda_{veg} = dh_v / \Delta S^2 h_v = d / \Delta S^2 = d \times N \qquad [14]$$

The equivalent wall roughness is schematically shown in Figure 4(b). It is assumed that the channel has the same hydraulic and geometrical dimensions as Figure 4(a) and the wall roughness has the same flow resistance force as the canopy drag. The wall shear stress τ_V equivalent to the canopy drag is defined in terms of the equivalent Manning's roughness coefficient n_V as

$$\tau_V = \frac{\rho g n_V^2 U^2}{R_0^{1/3\,1/3}} \qquad [15]$$

It is noted that τ_V is described by the depth-averaged velocity, U, since the flow is a single layer flow system.

4.2 Analytical procedure of n_V

Analysis of n_V consists of two computational steps.

(STEP-1) Giving channel geometry, vegetational properties, discharge Q_0 and water depth at the downstream boundary h_1, steady flow analysis for the real vegetated channel of Figure 4(a) is conducted by using the 2D2L model. Since h_1 is the first approximation for uniform flow depth, the solution does not always provide a uniform flow condition. h_1 must be renewed so that the water surface has the same hydraulic gradient as the bed slope I. Therefore, h_1 is modified iteratively until the water depth becomes uniform along the whole reach. The Newton-Raphson method of successive approximation is applied to obtain a solution for the uniform flow water depth h_0. After converging on the root, the water

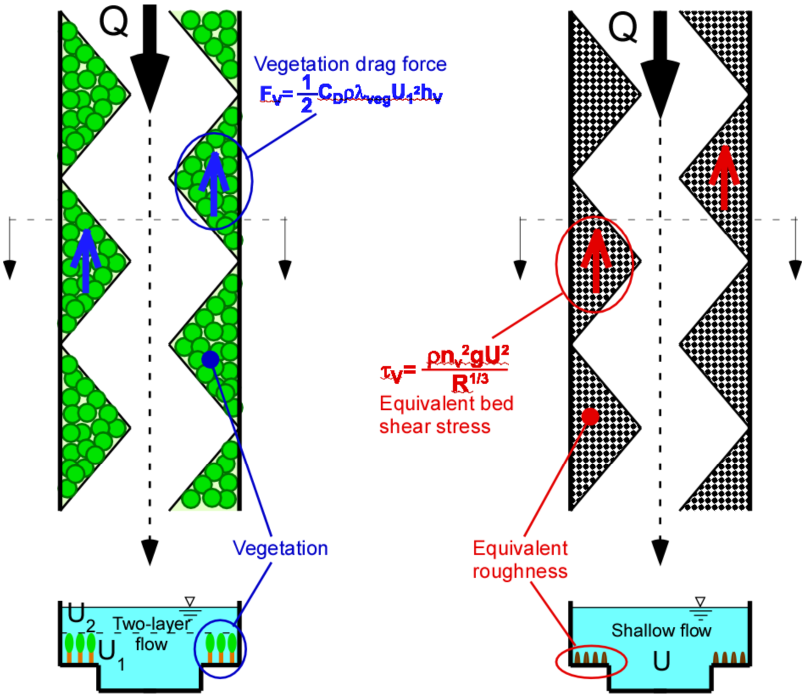

(a) Real channel with vegetated sandbar
[Two-layer flow]

(b) Virtual channel with equivalent roughness
[Single layer flow]

Figure 4. Open channels of compound cross section with vegetation or with equivalent wall roughness on alternatively arranged sandbar.

depth at the upstream boundary h_2 must be equal to h_1, which is to give the water depth of uniform flow h_0.

(STEP-2) Giving the first approximation of equivalent Manning's coefficient n_V, a steady flow analysis is carried out for a virtual channel of Figure 4(b) with discharge Q_0 and water depth at the downstream boundary h_0. This time, a conventional shallow flow model is used for the steady flow computation. Since the first approximation is not to give a solution of uniform flow, n_V should be modified until the hydraulic gradient becomes equal to the bed slope I or the water depth at the upstream boundary becomes h_0. The Newton-Raphson method is again applied to this iteration procedure. The final solution for n_V is provided after converging on the root.

The equivalent Manning's coefficient n_V computed in this manner is a concentrated hydraulic parameter in which all the dynamic components in Figure 4(a) are integrated. They are (i) vegetation canopy drag, F_V, (ii) vertical shear stress between flows over and through the vegetation, τ_i, (iii) horizontal shear stress between the vegetated area and main stream, τ_H, (iv) wall shear stress acting on the forest floor, τ_0 and (v) form drag force of channel meandering, F_G.

5. HYDRAULIC CONDITIONS IN THE ANALYSIS

5.1 Channel configuration

A uniform flow analysis was carried out to examine hydrodynamics in an open channel of compound cross section with vegetated sandbar or floodplain as schematically illustrated in Figure 5. For analytical simplicity, the meander profile of the main channel is approximated by triangle and vegetation is assumed to have uniform properties over the whole sandbar or floodplain. The channel width B and streamwise length of alternative bar λ_B are determined by referring to river morphology typically observed in middle-stream reaches in Japan (Muramoto and Fujita, 1977). The perimeters of the main channel and floodplain were kept constant along the longitudinal direction, which are equivalent to the dimensions of a straight open channel with compound cross section examined in the authors' previous study (Michioku et al., 2014). Wall roughness coefficient for each cross-sectional segment n_0 is assigned as listed in Table 3. The main channel depth is h_m=1m and the corresponding bank-full discharge for main channel is approximately Q_0≒100m^3/s. Refer to Tables 2 and 3 for other analytical conditions.

Table 2. Analytical conditions for vegetation.

<table>
<tr><th>CASE</th><th>Diameter
d (m)</th><th>Height
h_v (m)</th><th>Density
N (m⁻²)</th><th>Roughness density
λveg (m⁻¹)</th></tr>
<tr><td>0</td><td>0.1</td><td>4</td><td>0.1</td><td>0.01</td></tr>
<tr><td>1a</td><td>0.05</td><td rowspan="2">4</td><td rowspan="4">0.1</td><td>0.005</td></tr>
<tr><td>1b</td><td>0.2</td><td>0.02</td></tr>
<tr><td>2a</td><td rowspan="4">0.1</td><td>3</td><td>0.01</td></tr>
<tr><td>2b</td><td>5</td><td></td></tr>
<tr><td>3a</td><td rowspan="2">4</td><td>0.3</td><td>0.03</td></tr>
<tr><td>3b</td><td>0.5</td><td>0.05</td></tr>
</table>

Table 3. Analytical conditions for channel.

<table>
<tr><td>Discharge: Q (m³/s)</td><td colspan="2">200~4,000</td></tr>
<tr><td>Bed slope: I₀</td><td colspan="2">1/1,000</td></tr>
<tr><td rowspan="3">Manning's coefficient of wall roughness: n₀ (m⁻¹ᐟ³s)</td><td>Main channel</td><td>0.028</td></tr>
<tr><td>Floodplain (sandbar)</td><td>0.055</td></tr>
<tr><td>Forest floor</td><td>0.031</td></tr>
<tr><td rowspan="3">Morphology (m)</td><td>Main channel width</td><td>80.0</td></tr>
<tr><td>Main channel depth</td><td>1.0</td></tr>
<tr><td>Floodplain (sandbar) width</td><td>100</td></tr>
</table>

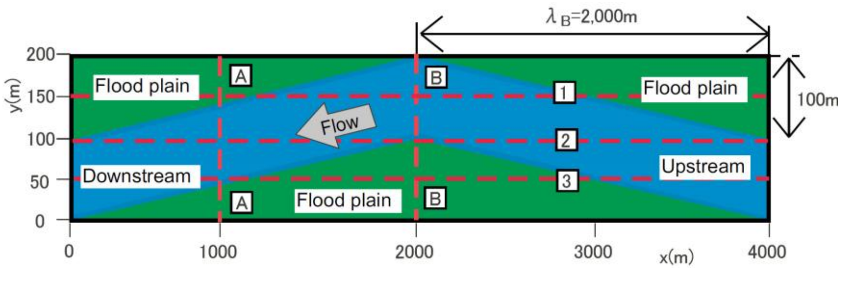

(a) Plane view of channel.

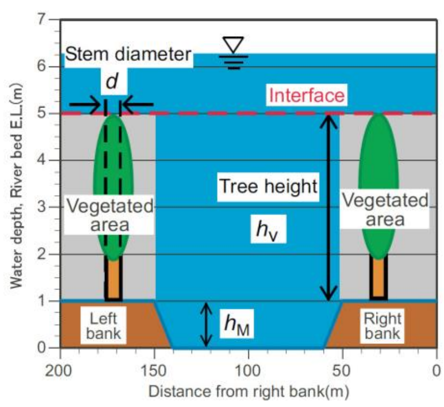

(b) Cross section "A-A".

Figure 5 Channel configuration for uniform flow analysis.

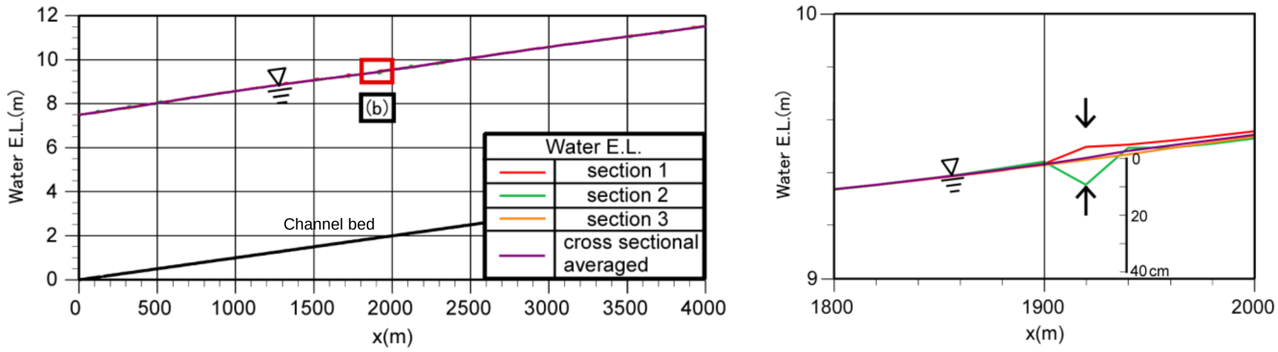

(a) Water surface profiles in the longitudinal cross sections 1, 2 and 3, where the locations are shown in Figure 5(a) .

(b) Enlargement of water surface profiles in the red rectangular in Figure 6(a).

Figure 6. Longitudinal profile of water surface for Q_0=4,000m^3/s in CASE-0.

5.2 Confirmation of uniform flow establishment

Strictly speaking, a uniform flow cannot be established in the present flow system, since it has a three dimensional flow field. However, the system must be approximated to a one-dimensional flow system in order to discuss Manning's roughness coefficient. In the present study, a uniform flow is defined as a state that the width averaged water depth h_0 is uniform in the streamwise direction. As mentioned in 4.2, the steady flow computation is iteratively executed by using the method of successive approximation until the water depth converges on h_0 along the whole reach.

In order to confirm if a "uniform flow" is established, the longitudinal profile of water surface in CASE-0 (Q_0=4,000m^3/s) is plotted in Figure 6. Solid lines in Figure 6(a) indicate water surface elevations in the longitudinal cross sections 1, 2 and 3 that is marked in Figure 5(a). Figure 6(b) shows an enlargement of the red rectangular zone in Figure 6(a), where a small standing wave is observed around the corner of the main channel meandering. The wave is infinitely small and the water surface is horizontal in the spanwise cross section. It is confirmed that the hydraulic gradient agrees with the bed slope and a uniform flow is completely established in the analysis.

6. FLOW FIELDS AND EQUIVALENT MANNING'S ROUGHNESS COEFFICIENT n_V

6.1 Flow structure

Figures 7 and 8 shows stream- and spanwise components of velocity (U, V) and entrainment velocity q_i in two cross sections, "A-A" and "B-B", respectively. The analytical conditions are for Q_0=4,000m^3/s in CASE-0. The cross sections are marked in broken lines in Figure 5(a). The entrainment is driven by shear stress at the interface between the upper and lower layers and it is responsible for the vertical exchange of mass and momentum between the two layers. q_i is calculated from the continuity equation as defined by Eq.[3]. The vertical momentum exchange due to entrainment are considered in the momentum balance in Eqs.[4] and [9].

It is seen both in Figures 7(a) and 8(a) that the depth-averaged velocity U is predominant in the main channel, whilst it is decelerated in the vegetated floodplain. The velocity difference between the main channel and the vegetated floodplain is a driving force of horizontal shear stress. Comparing velocities between the lower and upper layers, (U_1, U_2), in the figures, U_1 is always lower than U_2 in both cross sections, which generates vertical shear stress. The velocity is vertically homogeneous only in a very narrow area in front of the right bank as in Figure 8(a). It is confirmed that the two-layer flow structure is well preserved in a wide area of the channel and this is why the 2D2L model functions well in reproducing hydrodynamics in vegetated channels.

The spanwise components of velocity, (V_1, V_2), in Figures 7(b) and 8(b) suggests that, in both cross sections, the flow is directed from the vegetation to the main channel in the lower layer and it is in the opposite direction in the upper layer.

The entrainment velocity q_i in Figures 7(c) and 8(c) indicates that, in both cross sections, fluid in the vegetation is entrained into the upper layer, whilst entrainment in the main channel is downward. In this manner, the present analysis documents well how mass and momentum are exchanged between the vegetation and the main channel, as well as between the upper and lower layers.

6.2 Dependency of rating curve and equivalent Manning's roughness coefficient on vegetation properties

Figure 9 represents dependencies of rating curve, [Q_0.vs.h_0], and equivalent Manning's roughness coefficient, [Q_0.vs.n_V], on vegetation properties such as [d, h_v, N]. The white circle in each diagram corresponds to the hydraulic condition when the vegetation canopy starts to be submerged or the water surface is at the same level as the canopy top, i.e. h_0=h_M+h_v. Defining "submergence ratio" to be (h_0−h_M)/h_v, the submergence ratio is unity, i.e. (h_0−h_M)/h_v=1, in this situation. The figure provides general information on the channel's conveyance capacity in the vegetated channel.

Every diagram in Figure 9 shows that the increasing rate of water depth with discharge Q_0 is smaller for the submergent vegetation than for the emergent vegetation. The rating curve gradient discontinuously changes around the open circle, since a fraction of the projected area of vegetation to the whole cross section area is inversely proportional to water depth

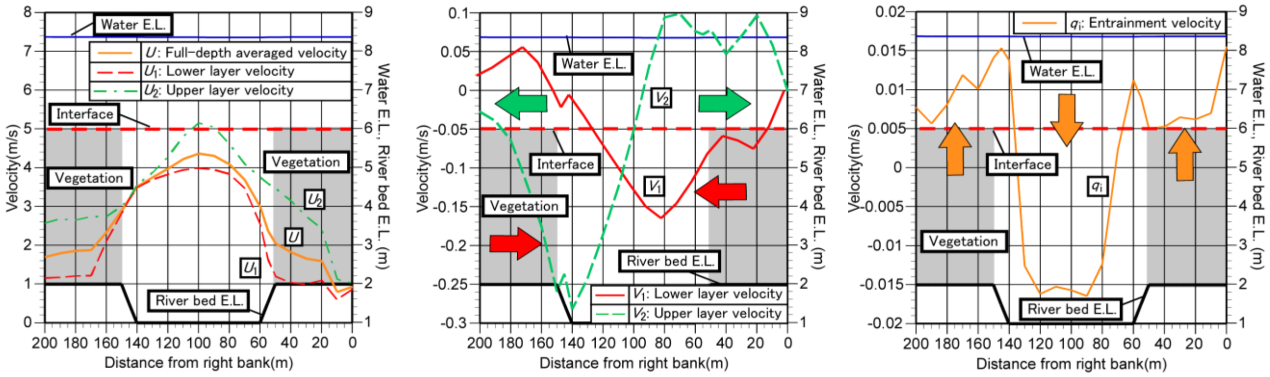

(a) Streamwise velocity (U_1, U_2, U) (b) Spanwise velocity (V_1, V_2) (c) Entrainment velocity q_i

Figure 7. Velocity profile in a spanwise cross section, "A-A", (Q_0=4,000m^3/s, CASE-0)

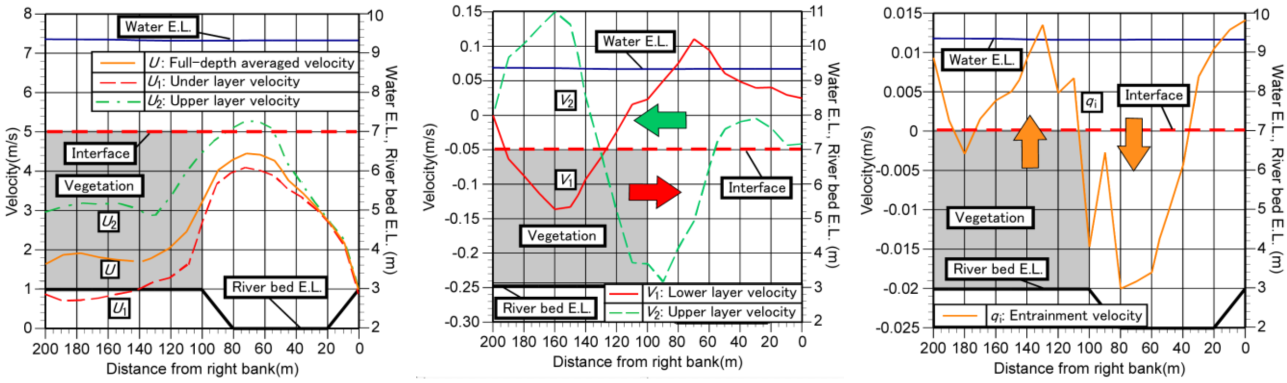

(a) Streamwise velocity (U_1, U_2, U) (b) Spanwise velocity (V_1, V_2) (c) Entrainment velocity q_i

Figure 8. Velocity profile in a spanwise cross section, "B-B", (Q_0=4,000m^3/s, CASE-0)

and discharge in the submerged vegetation, while it proportionally increases with discharge in the emergent vegetation. The functional dependency of n_V on Q_0 changes more remarkably before and after the vegetation submergence. n_V tends to be approximately constant independently of Q_0 for the submergent vegetation with higher discharge. Similar characteristics are recognized also in a straight channel (Michioku et al., 2014).

6.2.1 Rating curve: h_0 vs. Q_0

Figures 9(a) and 9(c) show how the conveyance capacity is influenced by stem diameter d and density N of vegetation, respectively. When the vegetation is emerged, i.e. $h_0<h_M+h_v$, increasing rate of h_0 against Q_0 is dependent on vegetation properties, [d, N]. On the other hand, the rating curves become parallel to each other and less dependent on [d, N] when the vegetation is submerged or $h_0 \geqq h_M+h_v$. They take approximately the same increasing rate of h_0 against Q_0 in this case.

Figure 9(b) represents influence of the vegetation height, h_v, on the channel conveyance capacity. Both in the rating curve and the relationship of n_V, all the cases for the emergent vegetation have a unique functional relationship of rating curve independently of h_v. On the contrary, the rating curve separates from each other depending on h_v after the vegetation is submerged. It is noteworthy that the gradient of the rating curve is approximately kept constant among the cases for the submergent canopy.

6.2.2 Dependency of n_v on Q_0

It is shown in the lower diagrams in Figures 9(a) to 9(c) that the equivalent Manning's roughness coefficient distributes in a range of n_v=0.031~0.20m$^{-1/3}$s, where n_0=0.031m$^{-1/3}$s is given as a boundary roughness coefficient of the vegetation floor. They coincide with a typical range of n_v frequently used in a one-dimensional flood flow analysis in prototype rivers. While n_v monotonically increases with Q_0 for the emergent vegetation, i.e. $h_0<h_M+h_v$, it becomes less dependent on Q_0 after taking a peak value for the submergence ratio of unity, i.e. $(h_0-h_M)/h_v$=1. For the submergent vegetation, a fraction of the blocked area by vegetation to the whole cross-sectional area is inversely proportional to discharge Q_0, whilst it linearly increases with Q_0 for the emergent vegetation. This is the reason why n_v takes a peak value for $(h_0-h_M)/h_v$=1 and the functional dependency between n_v and Q_0 shows an opposite tendency before and after vegetation submergence. With further increasing discharge after vegetation is submerged, a fraction of the frontal area of vegetation blocking the flow to the whole cross-sectional area gradually decreases and n_v asymptotically approaches a constant value independently of Q_0. In this regime of flow, n_v becomes dependent more on vegetation properties [d, h_v, N] and less

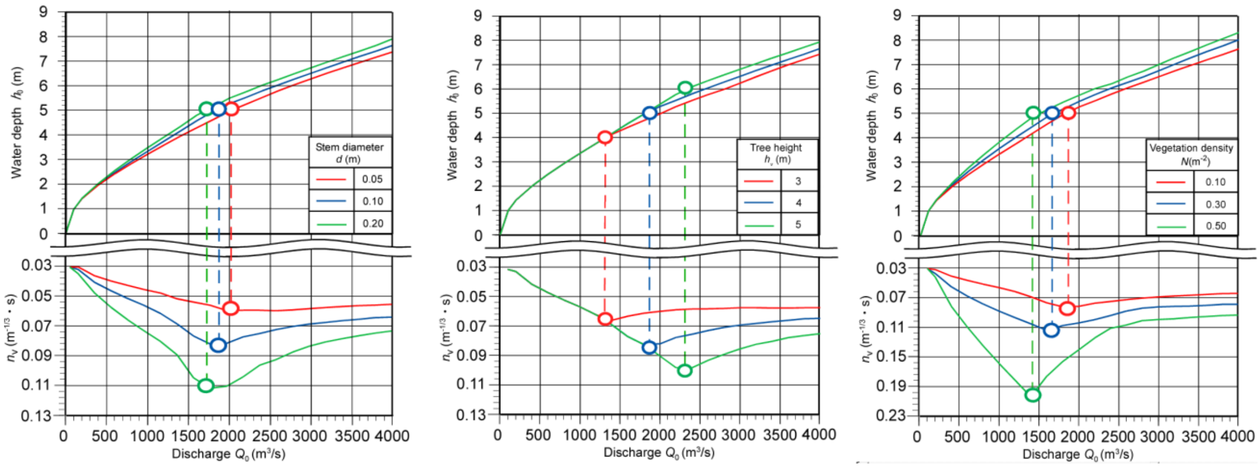

(a) Dependency on stem diameter d (b) Dependency on vegetation height h_v (c) Dependency on vegetation density N

Figure 9. Dependencies of rating curve, [Q_0.vs. h_0], and equivalent Manning's roughness coefficient, n_V, on vegetation properties [d, h_v, N].

dependent on discharge. Such a tendency is in agreement with previous studies done by Luhar and Nepf (2013) and Wu, Shen and Chou (1999).

7. FLOW RESISTANCE ANALYSIS

7.1 Form drag force of channel geometry and drag of vegetation canopy

In the present flow system, flow resistance consists of three components; (i) wall shear stress, (ii) form drag force due to channel geometry and (iii) vegetation canopy drag. The wall shear stress (i) is given by the original Manning's coefficient n_0 that has a constant value depending on the condition of channel bed surface. The form drag force (ii) is generated by meandering channel geometry. The vegetation drag (iii) is given by the drag force formula, Eq.[13]. Each component of flow resistance for CASE-0 in Table-2 is analyzed as below.

Let us assume four cases of channel. They are

- ■CASE-1A: with alternatively arranged and vegetated floodplain,
- ■CASE-1B: with alternatively arranged and bare floodplain,
- ■CASE-2A: with straight vegetated floodplain

and

- ■CASE-2B: with straight and bare floodplain.

CASE-1A is a reference case with the same conditions as CASE-0.

Referring to the field data, n_0=0.055$m^{-1/3}$s is used for the bare floodplain in CASE-1B and 2B (see Table-3).

Figure 10 represents analytical solutions for rating curve and n_v for the four cases. Note that solutions for n_v are shown only in the cases with vegetation or CASES-1A and 2A.

The four cases are aligned in the order of discharge of vegetation submergence (water depth of h_0=5m), as CASE-2B, -1B, -2A and -1A. CASE-1A is the case where both components of the channel's form drag and vegetation drag contribute to the flow resistance force, which takes the smallest flow conveyance capacity. Comparing CASE-2A and CASE-1B, the latter has a slightly larger capacity of flow conveyance than the former. Under hydraulic and vegetation conditions of the two cases, the vegetation drag more predominantly contributes to flow resistance than the channel's form drag does. Of course, the result might change depending on what conditions of vegetation and channel geometry are compared.

Through comparison of n_v between CASE-1A and -2A, the former takes larger n_v than the latter by about 0.01$m^{-1/3}$s. The difference between the two cases originates from turbulence and shear stresses generated by the three dimensional structure of channel geometry, which corresponds to the form drag component. It is noted again that all the three components of flow resistance, i.e. (i) wall shear stress, (ii) form drag force due to channel geometry and (iii) vegetation canopy drag are integrated in n_v in CASE-1A.

7.2 Composite roughness coefficient: N_2

In performing flood control management, a composite Manning's roughness coefficient N_2 is required to determine the channel's flow conveyance capacity. N_2 is a parameter describing average roughness of the channel and is computed by the following equation according to Ida (1960).

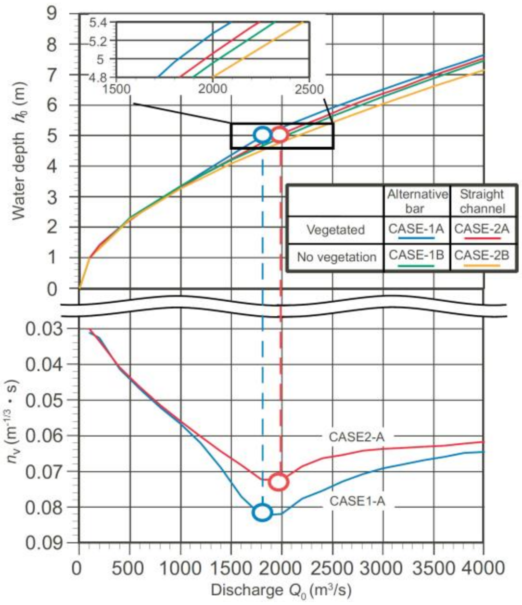

Figure 10. Rating curves, [Q_0.vs. h_0], and equivalent Manning's roughness coefficient, n_V for four different combinations of channel geometry and vegetation conditions.

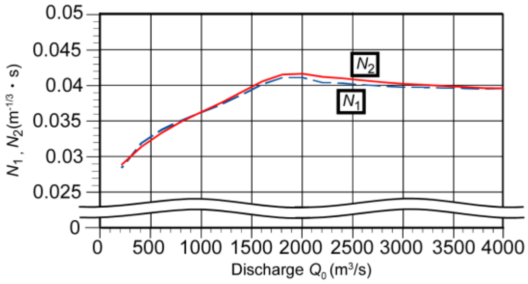

Figure 11. Composite Manning's roughness coefficient N_2 compared with the roughness coefficient in real flow N_1.

$$N_2 = \frac{\sum_{i=1}^{M}(A_i \cdot R_i^{2/3})}{\sum_{i=1}^{M}(A_i \cdot R_i^{2/3} / n_i)} \qquad [16]$$

where, A_i: cross-sectional area of the i-th segment (i=1,･･･, M）, M: number of sub-divided segments in the cross section, n_i: boundary roughness coefficient for the segment i and R_i: hydraulic radius of the segment i. n_V is applied as n_i for the vegetated perimeter.

Manning's roughness coefficient for the whole cross section N_1 is calculated from h_0 and Q_0 by using Eq.[12]. . As already mentioned in Figure 3, the 2D2L model can provide a very good estimation of N_1. Then, N_1 for CASE-1A is numerically computed by the model and compared with the composite roughness factor N_2.

N_1 and N_2 are in excellent agreement as shown in Figure 11. It is confirmed that the composite Manning's roughness coefficient N_2 can be precisely evaluated by giving an appropriate value of equivalent roughness factor n_V.

8. CONCLUSIONS

An equivalent Manning's roughness coefficient n_v corresponding to drag force of woody vegetation on alternatively arranged sandbar or floodplain was theoretically evaluated by the two-dimensional two-layer (2D2L) hydrodynamic model. Findings are summarized as follows.

i) In the 2D2L model, the flow consists of a fast flow over the vegetation canopy and the decelerated through-flow in the vegetation. A laboratory experiment was carried out in order to verify the model. The numerical solutions for the rating curve and Manning's roughness coefficient was in satisfactory agreement with the experimental data.

ii) A flow structure was investigated by preforming a numerical analysis of the 2D2L model. The analysis provided information on characteristic flow features such as acceleration and deceleration of fluid motions in and around the vegetation, mass and momentum exchanges between the main stream and vegetation, shear layers developed not only in horizontal but also in vertical directions and so on.

iii) When the vegetation was emerged, the frontal area of vegetation blocking the flow proportionally increased with increasing discharge. Therefore, n_v monotonically increased with discharge as long as vegetation was emerged.
iv) On the other hand, n_v gradually decreased with discharge after vegetation is submerged and then asymptotically approached a constant value independently of Q_0. In this flow regime, n_v is more dependent on vegetation properties such as stem diameter, vegetation density and height, etc., rather than on discharge.
v) Three components of flow resistance; (i) wall shear stress, (ii) form drag force due to channel geometry and (iii) vegetation canopy drag, were assumed and their individual contribution to the flow dynamics are investigated. Under the analytical conditions of hydraulics and vegetation in the present analysis, the vegetation drag more predominantly contributed to flow resistance than the channel's form drag force did.
vi) The composite Manning's roughness coefficient N_2 computed by using n_v provided an average roughness factor in agreement with the hydraulic gradient developed in the uniform flow.

ACKNOWLEDGMENTS

The study was financially supported by the Grant-in-Aid for Scientific Research (Project No. 26289164, Leader: Kohji Michioku).

REFERENCES

De Doncker, L., Troch, P., Verhoeven, R., Bal, K., Meire, P. and Quintelier J. (2009). Determination of the Manning roughness coefficient influenced by vegetation in the river Aa and Biebrza river, *Environ Fluid Mech.*, 9 (5), 549–567.

Folkard, A. (2011). Flow regimes in gaps within stands of flexible vegetation: Laboratory flume simulations, *Env. Fluid Mech.*, 11, 289–386.

Green, J.C. (2005). Comparison of blockage fac-tors in modelling the resistance of channels containing submerged macrophytes, *River Res Appl.*, 21(6), 671–86.

Hosoda T., Nagata N. and Muramoto Y. (1996). Numerical analysis of unsteady open channel flows by moving boundary tted coordinate system, *J. Hydraulic, Coastal and Environmental Engineering*, No.533/II-34, 267-272 (in Japanese).

Ida, Y. (1960): Steady flow in wide open channel. - on the effect of shape of its cross section, *Transactions of JSCE*, Np.69, Extra Press,(3-2), 1-18 (in Japanese).

Luhar, M. and Nepf, H. (2013). From the blade scale to the reach scale: A characterization of aquatic vegetative drag, *Adv. Water Resour.*, Vol.51, 305-316.

Michioku K., Nanjo M., Ishigaki T. and Maeno S. (2005). Two-dimensional analysis on solid-liquid-phase flow in and open channel with a rubble mound groin, *Proceedings of 31st IAHR Congress*, CD-ROM.

Michioku, K., Morioka N., Miyamoto H. and Akahori R. (2008). A two-layer model for analyzing flow field, bed shear stress and drag force in tree covered river channel, *Proc. 2nd International Symposium on Shallow Flows*, CD-ROM.

Michioku K., Kanda, K., Kometani, S., Irie, Y. and K. Yanagida and Uotani T. (2014). Analysis of equivalent Manning's roughness coefficient for trees vegetated on floodplain, *Proc. RIVER FLOW 2014*, 563-570.

Muramoto, Y. and Fujita, Y. (1977). Study on meso-scale river bed configuration, *Disaster Prevention Research Institute Annuals*, Kyoto University, 243-258 (in Japanese).

Nikora, V., Lamed, S., Nikora N., Debnath K., Cooper, G. and Reid, M. (2008). Hydraulic re-sistance due to aquatic vegetation in small streams: field study, *J Hydraulic Eng.*, ASCE, 134(9), 1326–1332.

Nezu I. and Nakagawa, H. (1993). Turbulence in Open Channel Flows, *IAHR Monograph*, Balkema, 281p.

Nepf H. M. (1999). Drag Turbulence, and diffusion in flow through emergent vegetation, *Water Resources Research*, Vol.35-2, 479-489.

Nikora, N. and Nikora, V. (2007). A viscous drag concept for flow resistance in vegetated channels, *Proc. 32nd IAHR Congress*, Venice, CD-ROM.

Wu, F., Shen, H. and Chou, Y. (1999). Variation of roughness coefficients for unsubmerged and submerged vegetation, *J. Hydraulic Eng.*, 125(9), 34–942.